Thermochimica Acta, 182 (1991) 209–217
Elsevier Science Publishers B.V., Amsterdam

Systematics on the thermal reactions of lanthanide malonates $Ln_2(C_3H_2O_4)_3 \cdot nH_2O$ in the solid state

Kazuo Muraishi

Department of Chemistry, Faculty of Science, Yamagata University, Koshirakawa, Yamagata 990 (Japan)

Hiroko Yokobayashi and Kenzo Nagase

College of General Education, Tohoku University, Kawauchi, Sendai 980 (Japan)

(Received 8 October 1990)

Abstract

The thermal reactions of the lanthanide malonates in the solid state were investigated systematically by means of TG/DTA, and X-ray, IR and elemental analyses. The onset temperatures of the dehydration (t_h) and decomposition (t_d), which can measure relative stabilities of the hydrated and anhydrous malonates, respectively, varied systematically with some physical parameters of the lanthanides and lanthanide malonates.

INTRODUCTION

The thermal decomposition reactions of lanthanide carboxylates have been studied with interest both in analytical chemistry and in inorganic and coordination chemistry [1]. The malonate ion is characterised by a fairly active methylene group and in making a stable six-membered chelate ring with a lanthanide ion Ln^{3+} [2]. It is of interest to know how these properties affect the thermal properties of its compound with Ln^{3+} and to compare the thermal data with those of other dicarboxylates.

The present work reports the TG/DTA, X-ray and IR measurements for all the starting samples and/or their decomposition products to find any systematic behaviour of their thermal properties.

EXPERIMENTAL

The preparation of the lanthanide malonate hydrates, and the apparatus and procedures used were the same as those described in our previous paper [3]. The TG–DTA curves were recorded simultaneously at a heating rate of $3°C\ min^{-1}$ in atmospheres of nitrogen flowing at 60 ml min^{-1} and static

0040-6031/91/$03.50

air. Each measurement used about 10 mg of powdered sample which was placed in a platinum crucible.

RESULTS AND DISCUSSION

TG / DTA curves and physical measurements of $Ln_2(C_3H_2O_4)_3 \cdot n H_2O$

The TG/DTA curves of the malonates of La–Lu obtained in N_2 and air are shown in Figs. 1 and 2. The weight-loss steps observed below 200 °C correspond to the dehydration course. The dehydration modes can be classified into three groups: La, Ce–Eu and Gd–Lu. This classification coincided with that of the IR spectral and X-ray patterns, typical examples of which are shown in Figs. 3 and 4, respectively.

The decomposition of the anhydrous malonates proceeds following a TG plateau. The process of decomposition depended on the ambient atmosphere (N_2, air). The intermediate and final products estimated from TG, IR, X-ray and elemental analyses are given in Table 1.

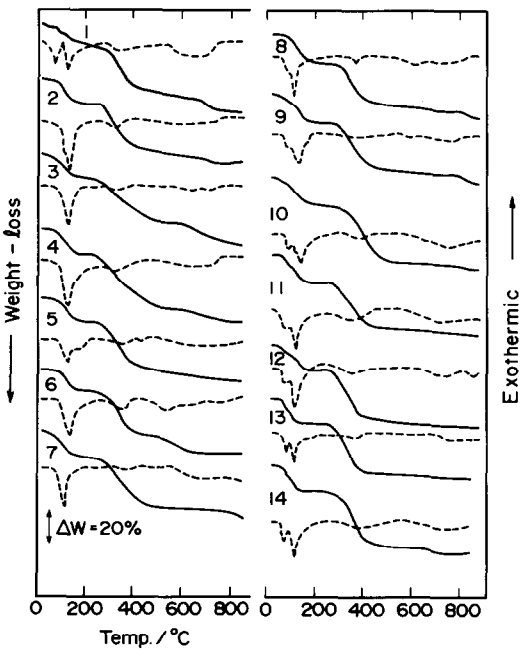

Fig. 1. TG–DTA curves of (1) $La_2(C_3H_2O_4)_3 \cdot 5H_2O$, (2) $Ce_2(C_3H_2O_4)_3 \cdot 6H_2O$, (3) $Pr_2(C_3H_2O_4)_3 \cdot 6H_2O$, (4) $Nd_2(C_3H_2O_4)_3 \cdot 6H_2O$, (5) $Sm_2(C_3H_2O_4)_3 \cdot 6H_2O$, (6) $Eu_2(C_3H_2O_4)_3 \cdot 6H_2O$, (7) $Gd_2(C_3H_2O_4)_3 \cdot 8H_2O$, (8) $Tb_2(C_3H_2O_4)_3 \cdot 8H_2O$, (9) $Dy_2(C_3H_2O_4)_3 \cdot 8H_2O$, (10) $Ho_2(C_3H_2O_4)_3 \cdot 8H_2O$, (11) $Er_2(C_3H_2O_4)_3 \cdot 8H_2O$, (12) $Tm_2(C_3H_2O_4)_3 \cdot 8H_2O$, (13) $Yb_2(C_3H_2O_4)_3 \cdot 8H_2O$ and (14) $Lu_2(C_3H_2O_4)_3 \cdot 8H_2O$ in flowing nitrogen: ———, TG; - - - - - -, DTA.

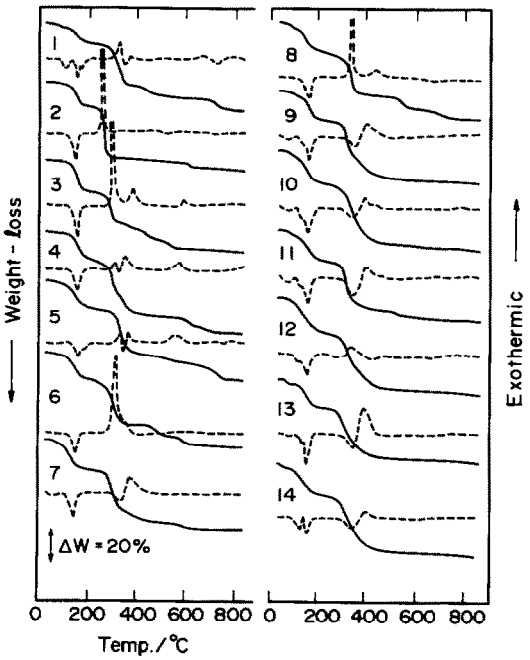

Fig. 2. TG–DTA curves of (1) $La_2(C_3H_2O_4)_3 \cdot 5H_2O$, (2) $Ce_2(C_3H_2O_4)_3 \cdot 6H_2O$, (3) $Pr_2(C_3H_2O_4)_3 \cdot 6H_2O$, (4) $Nd_2(C_3H_2O_4)_3 \cdot 6H_2O$, (5) $Sm_2(C_3H_2O_4)_3 \cdot 6H_2O$, (6) $Eu_2(C_3H_2O_4)_3 \cdot 6H_2O$, (7) $Gd_2(C_3H_2O_4)_3 \cdot 8H_2O$, (8) $Tb_2(C_3H_2O_4)_3 \cdot 8H_2O$, (9) $Dy_2(C_3H_2O_4)_3 \cdot 8H_2O$, (10) $Ho_2(C_3H_2O_4)_3 \cdot 8H_2O$, (11) $Er_2(C_3H_2O_4)_3 \cdot 8H_2O$, (12) $Tm_2(C_3H_2O_4)_3 \cdot 8H_2O$, (13) $Yb_2(C_3H_2O_4)_3 \cdot 8H_2O$ and (14) $Lu_2(C_3H_2O_4)_3 \cdot 8H_2O$ in static air: ———, TG; - - - - - -, DTA.

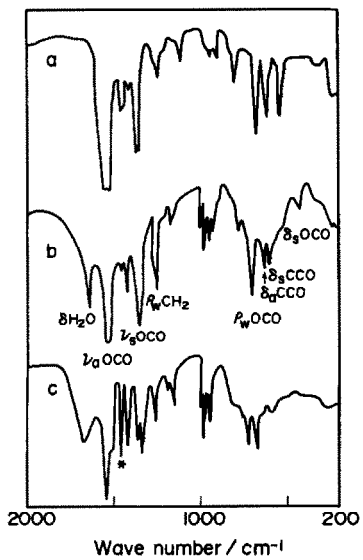

Fig. 3. Infrared spectra of (a) $La_2(C_3H_2O_4)_3 \cdot 5H_2O$, (b) $Ce_2(C_3H_2O_4)_3 \cdot 6H_2O$ and (c) $Tm_2(C_3H_2O_4)_3 \cdot 8H_2O$; *, active methylene.

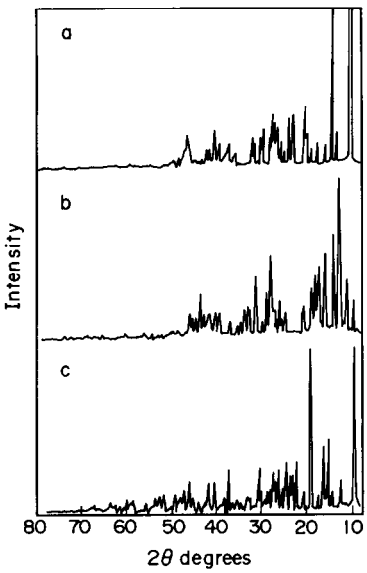

Fig. 4. X-ray powder diffraction patterns of (a) $La_2(C_3H_2O_4)_3 \cdot 5H_2O$, (b) $Ce_2(C_3H_2O_4)_3 \cdot 6H_2O$ and (c) $Tm_2(C_3H_2O_4)_3 \cdot 8H_2O$.

Dehydration course

According to the X-ray structural analysis, the hexahydrates (Ce–Eu) have two kinds of malonate ion: a chelated ion and an open, bridging ion. However, all malonate ions in the octahydrates (Gd–Lu) are chelated. It is known that relative covalencies in the metal–carboxylate oxygen bond of metal carboxylates can be estimated by measuring the separations ($\Delta\nu$) in frequency between $\nu_{asym}(OCO)$ and $\nu_{sym}(OCO)$ of their IR spectra [4]. Therefore, the relationship between $\Delta\nu$ and the ionic radius of Ln^{3+} (r) for the malonates was examined (Fig. 5). The covalencies of the hexahydrates were almost independent of r, whereas those of the octahydrates increased with decreasing r. In the case of the hexahydrates, therefore, the decrease in r (the increase in effective charge of Ln^{3+}) presumably strengthens the Ln^{3+}–OH_2 bond rather than the Ln^{3+}–O(mal) bond.

The separation values and dehydration temperatures (t_h) of lanthanide malonate hydrates in a flowing nitrogen atmosphere are given in Table 2. The relationship between the Ln–O(mal) and Ln–OH_2 bonds was examined by plotting the separation, $\Delta\nu$, against the dehydration temperatures which gives the relative strengths of the Ln–OH_2 bonds (Fig. 6). It is clear that the Ln–OH_2 bond becomes weak as the Ln^{3+}–O(mal) bond becomes strong. Figure 6 shows two straight lines with different slopes; this is understandable — both groups have different structures and different numbers of H_2O molecules.

TABLE 1

Initial weight-loss temperatures (t_d), DTA peak temperatures (t_m) and weight-loss values (ΔW) for the decomposition of anhydrous lanthanoid malonates in a flowing nitrogen atmosphere

Malonate	Decomposition				
	t_d (°C)	t_m (°C)	ΔW_{obsd} (%)	ΔW_{calcd} (%)	Product
$La_2(C_3H_2O_4)_3$	250	325	30.2	31.8	$La_2O_2CO_3$
	607	–	37.9	38.3	La_2O_3
$Ce_2(C_3H_2O_4)_3$	240	325	31.3	30.8	$Ce_2O_2CO_3$
	616	–	35.8	34.9	Ce_2O_3
$Pr_2(C_3H_2O_4)_3$	247	329	29.6	30.8	$Pr_2O_2CO_3$
	617	–	35.8	34.9	Pr_2O_3
$Nd_2(C_3H_2O_4)_3$	249	330	29.7	30.5	$Nd_2O_2CO_3$
	618	–	37.1	36.7	Nd_2O_3
$Sm_2(C_3H_2O_4)_3$	253	340	29.2	29.9	$Sm_2O_2CO_3$
	618	–	35.9	36.1	Sm_2O_3
$Eu_2(C_3H_2O_4)_3$	249	342	31.9	29.8	$Eu_2O_2CO_3$
	620	–	37.8	35.9	Eu_2O_3
$Gd_2(C_3H_2O_4)_3$	229	338	29.1	28.0	$Gd_2O_2CO_3$
	640	–	34.3	33.8	Gd_2O_3
$Tb_2(C_3H_2O_4)_3$	232	337	27.5	27.9	$Tb_2O_2CO_3$
	648	–	33.7	33.6	Tb_2O_3
$Dy_2(C_3H_2O_4)_3$	234	338	27.8	27.6	$Dy_2O_2CO_3$
	654	–	33.9	33.3	Dy_2O_3
$Ho_2(C_3H_2O_4)_3$	237	338	29.2	27.5	$Ho_2O_2CO_3$
	656	–	33.2	33.1	Ho_2O_3
$Er_2(C_3H_2O_4)_3$	238	333	25.9	27.3	$Er_2O_2CO_3$
	652	–	30.0	32.9	Er_2O_3
$Tm_2(C_3H_2O_4)_3$	240	334	27.8	27.2	$Tm_2O_2CO_3$
	654	–	33.0	32.8	Tm_2O_3
$Yb_2(C_3H_2O_4)_3$	238	334	28.3	26.9	$Yb_2O_2CO_3$
	660	–	31.7	32.4	Yb_2O_3
$Lu_2(C_3H_2O_4)_3$	242	343	29.6	26.8	$Lu_2O_2CO_3$
	660	–	32.2	32.3	Lu_2O_3

Decomposition course

The decomposition of the anhydrous malonates was influenced by the ambient atmospheres. In the case of the lighter lanthanides, except for Ce, the decomposition temperatures (t_d) were somewhat lower in N_2 than in air, whereas the t_d values for the heavier lanthanides were higher in N_2 than in air. The decomposition of the Ce compound was strongly dependent on the atmosphere and its t_d in air was much lower, as has been reported in the case of the oxalates [5].

In N_2 (inert atmosphere), the decomposition process can be expressed as

$$Ln_2(C_3H_2O_4)_3 \rightarrow Ln_2O_2CO_3 \rightarrow Ln_2O_3 \quad (1)$$

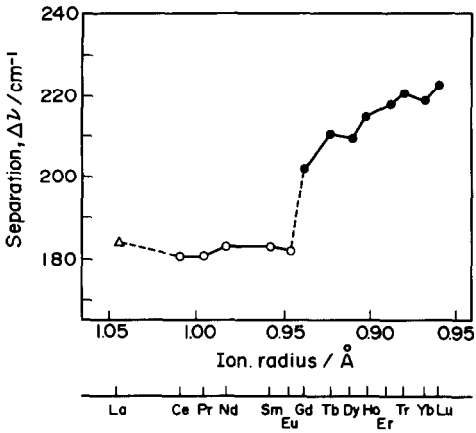

Fig. 5. Relation between the separation ($\Delta\nu = \nu_{asym}(OCO) - \nu_{sym}(OCO)$) and ion radius of lanthanide.

although there is some evidence of other products before the formation of $Ln_2O_2CO_3$. For all the lanthanides the formation of $Ln_2O_2CO_3$ is implied from the weight-loss values, elemental analyses and IR spectra. X-ray identification was not useful, because the products were X-ray amorphous except for the final products, Ln_2O_3. The final products for the lighter lanthanides were light grey in colour, indicating the presence of a small amount of dispersed elementary carbon, whereas the final products from the heavier lanthanides were black, indicating that a considerable amount of

TABLE 2

The separation values ($\Delta\nu$) and initial dehydration temperatures (t_h) of lanthanoid malonate hydrates in a flowing nitrogen atmosphere

Malonate	$\nu_{asym}(OCO)$ (cm^{-1})	$\nu_{sym}(OCO)$ (cm^{-1})	$\Delta\nu$ (cm^{-1})	t_h (°C)
$La_2(C_3H_2O_4)_3 \cdot 5H_2O$	1551	1368	183	76
$Ce_2(C_3H_2O_4)_3 \cdot 6H_2O$	1562	1382	180	81
$Pr_2(C_3H_2O_4)_3 \cdot 6H_2O$	1560	1380	180	89
$Nd_2(C_3H_2O_4)_3 \cdot 6H_2O$	1562	1380	182	87
$Sm_2(C_3H_2O_4)_3 \cdot 6H_2O$	1562	1380	182	83
$Eu_2(C_3H_2O_4)_3 \cdot 6H_2O$	1564	1383	181	82
$Gd_2(C_3H_2O_4)_3 \cdot 8H_2O$	1572	1371	201	59
$Tb_2(C_3H_2O_4)_3 \cdot 8H_2O$	1572	1362	210	54
$Dy_2(C_3H_2O_4)_3 \cdot 8H_2O$	1571	1362	209	59
$Ho_2(C_3H_2O_4)_3 \cdot 8H_2O$	1571	1357	214	57
$Er_2(C_3H_2O_4)_3 \cdot 8H_2O$	1570	1353	217	53
$Tm_2(C_3H_2O_4)_3 \cdot 8H_2O$	1575	1355	220	58
$Yb_2(C_3H_2O_4)_3 \cdot 8H_2O$	1573	1355	218	54
$Lu_2(C_3H_2O_4)_3 \cdot 8H_2O$	1576	1354	222	52

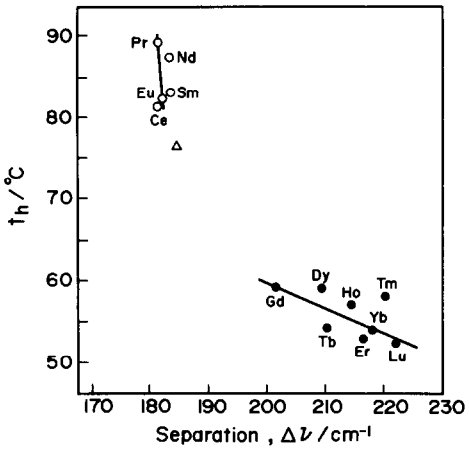

Fig. 6. Relation between initial weight-loss dehydration temperatures (t_h) and the separation of lanthanide malonates: ○ and • indicate the lighter and heavier lanthanide malonate hydrates, respectively.

elementary carbon had been formed by the disproportionation of carbon in the valence state.

From the TG curves, it appears that it is easier for the lighter lanthanides to form oxycarbonates. The reason may be that carbonate ion is a soft base and therefore favours a soft acid, in other words, a larger lanthanide ion. The onset temperatures of decomposition for the lighter lanthanides (La–Eu) were almost independent of the atomic numbers of Ln. A drop in t_d for Ce may be correlated to the tendency to form Ce^{4+}. In the heavier lanthanides, however, t_d tended to increase with increasing atomic number of Ln. In other words, the stability of the malonates increased with increasing effective nuclear charge of Ln^{3+}. This is very unusual because numerous experimental results suggest that the carboxylates decompose at lower temperatures as the interaction energies of metal–carboxylate oxygen increase. For a number of metal oxalates, Kahwa and Mulokozi [6] have demonstrated a perfect linear relationship of negative slope between t_d and the interaction energies evaluated by

$$t_d = 516 - 1.4006(r_c/r_i)\sqrt{\sum I_i} \qquad (2)$$

where r_c, r_i and ΣI_i denote the covalent radii, ionic radii and total sums of ionization potentials of the metals [7], respectively.

The plot of t_d against Kahwa's parameter for the malonates of the heavier lanthanides is shown in Fig. 7: a straight line was obtained but its slope is positive. This positive slope is in conflict with the mechanism in which the carboxylate decomposition is initiated by C–O bond-breaking, suggesting that another mechanism characteristic of the malonate is occurring. A hydrogen atom in the methylene group between two electron-attracting

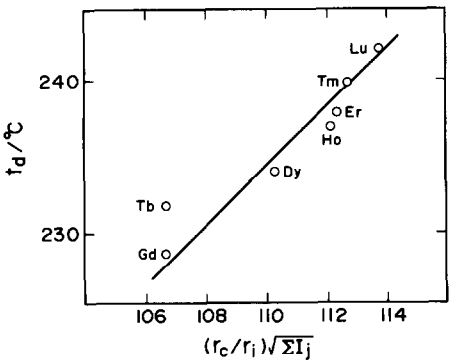

Fig. 7. Relation between initial decomposition temperatures (t_d) in flowing nitrogen and the ratio $(r_c/r_i)\sqrt{\Sigma I_i}$ of the heavier lanthanides.

carboxyl groups is known to be highly activated and acts like proton. The activation is expected to be enhanced as the effective nuclear charge of the lanthanide ion increases. Therefore, the mechanism suggested by Shishido and Ogasawara [8] for the alkaline metal malonates, in which the decomposition of malonate is initiated by the deprotonation of the methylene group, seems likely for the heavier lanthanides. In the infrared spectra of the heavier lanthanides, the absorption peak near 1400 cm^{-1}, which is due to the activated methylene, has a high intensity, compared with the lighter lanthanides.

An anomalous drop in t_d was observed for Yb, which may be attributed to the tendency to form Yb^{2+}.

A major difference in the DTA curves in air compared with those in N_2 was observed for Ce, Pr, Eu, Tb and Yb. The DTA curves of these lanthanides in air were characterized by a very sharp and/or strong exotherm at the initial stage of the decomposition. Ce, Pr and Tb can form +4 oxidation states, and Eu and Yb can form +2 oxidation states [9]. The existence of +2 and +4 oxidation states have been ascribed simply to the extra stability associated with the formation of empty $4f^0(Ce^{4+})$, half-filled $4f^7(Eu^{2+}, Tb^{4+})$ and filled $4f^{14}(Yb^{2+})$ subshells, although this argument is unconvincing in the case of $Pr^{4+}(4f^1)$.

It can therefore be presumed that the changes in oxidation state are responsible for the DTA exotherms. It is well known that metal oxalates evolve carbon monoxide when the metals move to higher oxidation states: the combustion of CO with O_2 produces the strong exotherm in the DTA curve. Because it is difficult to imagine that CO is evolved from carboxylates when the metals move to lower oxidation states, in the cases of Eu and Yb malonates, CO might be evolved in the consecutive stages: Ln^{3+} may first be reduced to Ln^{2+} by malonate ion and then reoxidized to Ln^{3+} with an oxidizing product, in the latter stage of which CO is evolved. In fact, the

endotherms observed for Eu and Yb were much broader than the sharp peaks for Ce, Pr and Tb.

REFERENCES

1 Beilsteins Handbuch der Organischen Chemie, Bd 2/3, Springer-Verlag, Berlin, 1976, Syst. Nr. 171, p. 1874; Gmelins Handbuch der Anorganischen Chemie, Sc, Y, La–Lu, D5, Carboxylates, Springer, Berlin, 1984, p. 150.
2 E. Hansson, Acta Chem. Scand., 27 (1973) 2827.
3 K. Muraishi, K. Nagase, M. Kikuchi, K. Sone and N. Tanaka, Bull. Chem. Soc. Jpn., 55 (1982) 1845.
4 A. Carillo, P. Vieles and A. Banniol, C.R. Acad. Sci., Ser. C, 274 (1972) 912; D.K. Koppikar and S. Soundarajan, Monatsh. Chem., 107 (1976) 105; M.Y. Al-Janabi, N.J. Ali, N.E. Milad and M.M. Barbooti, Thermochim. Acta, 25 (1978) 101; M.A. Nabar and B.N. Jukar, Bull. Chem. Soc. Jpn., 58 (1985) 3582; P.V. Khadikar, S.M. Ali and B. Heda, J. Therm. Anal., 30 (1985) 305.
5 M.J. Fuller and J. Pinkstone, J. Less-Comm. Metals, 70 (1980) 127.
6 I.A. Kahwa and A.M. Mulokozi, J. Therm. Anal., 22 (1981) 61; J. Therm. Anal., 24 (1982) 265.
7 C.E. Moore, Analysis of Optical Spectra, NSRDS-NBS 34, NBS (1971); P.V. Parish. The Metallic Elements. Longmans, London, 1977, Appendix A; R.C. Weast, Handbook of Chemistry and Physics, Vol. 61, CRC Press, Boca Raton, 1980, p. E-69.
8 S. Shishido and A. Ogasawara, Sci. Rep. Niigata Univ., Ser. C, 3 (1971) 23.
9 F.A. Cotton and G. Wilkinson, Advanced Inorganic Chemistry, Wiley–Interscience, New York, 5th edn., 1988.